INFECTION AND IMMUNITY, Feb. 2005, p. 695–702 Vol. 73, No. 2
0019-9567/05/$08.00+0 doi:10.1128/IAI.73.2.695–702.2005

Bioluminescence Imaging of *Toxoplasma gondii* Infection in Living Mice Reveals Dramatic Differences between Strains

Jeroen P. J. Saeij,[1]† Jon P. Boyle,[1]† Michael E. Grigg,[1,2] Gustavo Arrizabalaga,[1]‡ and John C. Boothroyd[1]*

Department of Microbiology and Immunology, Stanford University School of Medicine, Stanford, California,[1] *and Department of Medicine, University of British Columbia, Vancouver, British Columbia, Canada*[2]

Received 17 August 2004/Returned for modification 22 September 2004/Accepted 11 October 2004

We examined the in vivo growth, dissemination, and reactivation of strains of the protozoan parasite *Toxoplasma gondii* using a bioluminescence-based imaging system. Two *T. gondii* strains, one with a highly virulent disease phenotype in mice (S23) and the other with a 1,000-fold-lower virulence phenotype (S22), were engineered to stably express the light-emitting protein luciferase. One clone of each wild-type strain was isolated, and the two clones (S23-luc7 and S22-luc2) were found to express similar levels of luciferase. Mice were infected intraperitoneally with S23-luc7 (50 or 5 parasites) or S22-luc2 (500, 50, or 5 parasites), and the progress of the infections was examined noninvasively following injection of the substrate for luciferase, D-luciferin. In mice infected with 50 S23-luc7 parasites, the parasites grew exponentially within the peritoneal cavity (as measured by light emitted from luciferase-expressing parasites) during days 1 to 10 p.i., and this proliferation continued until there was severe disease. In mice infected with 500 S22-luc2 parasites, the parasites proliferated in a fashion similar to the S23-luc7 proliferation during days 1 to 6, but this was followed by a precipitous drop in the signal to levels below the limit of detection. Using this technique, we were also able to observe the process of reactivation of *T. gondii* in chronically infected mice. After treatment with dexamethasone, we detected reactivation of toxoplasmosis in mice infected with S23-luc7 and S22-luc2. During reactivation, growth of S23-luc7 was initially detected primarily in the head and neck area, while in S22-luc2-infected mice the parasites were detected primarily in the abdomen. This method has great potential for identifying important differences in the dissemination and growth of different *T. gondii* strains, especially strains with dramatically different disease outcomes.

Toxoplasma gondii is an obligate intracellular parasite that is able to infect virtually any nucleated cell from a wide range of mammalian and avian species (12). In humans, *Toxoplasma* infections are widespread and can lead to severe disease in individuals with immature or suppressed immune systems. Consequently, toxoplasmosis became one of the major opportunistic infections of the AIDS epidemic (14). Acute infection, which is associated with the rapidly dividing form or tachyzoite, is normally controlled by innate and adaptive immune responses. Sterile immunity is not achieved, however, and instead an asymptomatic, chronic phase of infection ensues. The parasite persists by differentiating into bradyzoites, a form that expresses surface antigens that are distinct from those of tachyzoites. The bradyzoites exist within cysts that remain in the host for long periods in less immunologically active tissues, such as the central nervous system, apparently impervious to the robust immune response induced by the tachyzoite stages (6, 11, 22).

The outcome of toxoplasmosis in the mouse model is strongly dependent on the infecting *T. gondii* strain. The majority of *T. gondii* strains comprise three distinct clonal lineages (20) and differ genetically by 1% or less (24). Strains with the type I genotype are highly virulent in mice, and regardless of the genetic background of the mouse host, the lethal dose is a single viable parasite. In contrast, type II and III strains have 50% lethal doses (LD_{50}s) of $>10^3$ parasites, and the precise outcome of infection is dependent on the genotype of the host. The virulence of type I strains is in part a result of their enhanced migration and higher growth rates, which allow them to disseminate more rapidly (2) and reach higher tissue burdens, which ultimately leads to a cascade of proinflammatory mediators that induce pathology (8, 17). Recently, we reported that a cross between the less virulent type II strain ME49 and the type III strain CEP can give rise to progeny with enhanced virulence (9). One of the F1 progeny, designated S23, has an LD_{50} that is at least 3 logs lower than that of either parent.

To investigate the biological basis for this enhanced virulence, we compared the dissemination of S23 in mice with the dissemination of one of its nonvirulent siblings, S22 (9). To do this, we engineered the two strains to express firefly luciferase. The resulting bioluminescent strains were then used to determine the spatiotemporal distribution of infection of each strain in mice. Using this method, we observed both qualitative and quantitative differences in the dissemination patterns of the two strains. We were also able to use this technique to observe the time course of reactivation induced by immunosuppressants.

* Corresponding author. Mailing address: Department of Microbiology and Immunology, Fairchild Building D305, Stanford University School of Medicine, 300 Pasteur Dr., Stanford, CA 94305-5124. Phone: (650) 723-7984. Fax: (650) 723-6853. E-mail: john.boothroyd@stanford.edu.

† J.P.J.S. and J.P.B. contributed equally to this article.

‡ Present address: Department of Microbiology, Molecular Biology, and Biochemistry, University of Idaho, Moscow, Idaho.

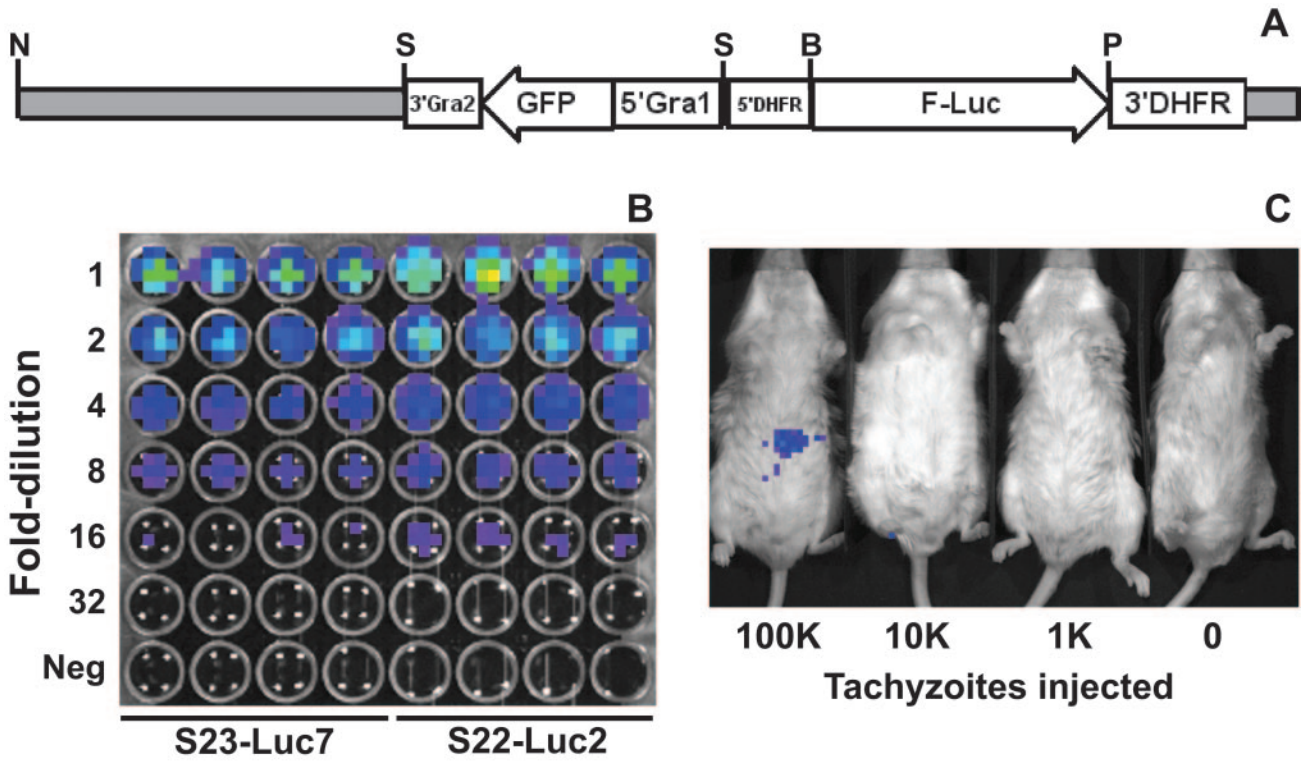

FIG. 1. (A) Construct used to generate luciferase-expressing *T. gondii* clones S23-luc7 and S22-luc2. pDHFR-Luc (obtained from David Roos, University of Pennsylvania), a plasmid with a pBluescript KS(−) backbone and the firefly luciferase gene driven by the *T. gondii DHFR* promoter, was modified by addition of a GFP expression cassette driven by the GRA1 promoter. The plasmid was linearized with NotI prior to transfection. Enzyme abbreviations: N, NotI; S, SalI; B, BglII; P, PstI. (B) Dilution of S23-luc7 and S22-luc2 tachyzoites, demonstrating the similar levels of light production in the presence of D-luciferin. Freshly harvested tachyzoites were quantified and serially diluted in twofold increments in 96-well plates with black walls in quadruplicate. D-Luciferin was added, and each plate was imaged 10 min later. The topmost wells contained 5×10^5 tachyzoites. In the pseudocolor images the luciferase photon intensity ranges from the lowest intensity (blue) to the highest intensity (red). (C) S22-luc2 tachyzoites were serially diluted in 10-fold increments, and different amounts were injected intraperitoneally into BALB/c mice. Luciferin was injected immediately after this, and 10 min later mice were imaged as described in Materials and Methods. The minimum number of tachyzoites necessary to detect a bioluminescent signal greater than the background signal in these experiments was between 10,000 and 100,000.

MATERIALS AND METHODS

Parasites. Strains were maintained in vitro by serial passage on monolayers of human foreskin fibroblasts (HFFs) at 37°C in the presence of 5% CO_2 as previously described (19). HFFs were grown in Dulbecco modified Eagle medium (GIBCO BRL) supplemented with 10% NuSerum (Collaborative Biomedical Products), 2 mM glutamine, 50 μg of penicillin per ml, 50 μg of streptomycin per ml, and 20 μg of gentamicin per ml. S23 is the virulent offspring of two relatively avirulent parents, ME49 and CEP. S22 is the genetically most similar (21) but less virulent sibling of S23 (9).

Generation of bioluminescent *T. gondii*. Plasmid pDHFR-Luc was provided by David Roos (University of Pennsylvania). This plasmid has the firefly luciferase coding sequence (GenBank accession no. P08659) (except for the last three codons) cloned behind the promoter and the 5′ untranslated region (UTR) of the *T. gondii* gene for dihydrofolate reductase (DHFR) (positions 933 to 1383 of the gene; GenBank accession no. L08489). The luciferase coding sequence was followed by the 3′ UTR from DHFR (positions 7792 to 8175) (Fig. 1A). This construct was modified by insertion of a green fluorescent protein (GFP) expression cassette into the SalI restriction site. The GFP cassette contained the promoter and 5′ UTR sequence from the *T. gondii* GRA1 gene (positions 8 to 612 of the gene; GenBank accession no. M26007) and the 3′ region from the *T. gondii* GRA2 gene (positions 1179 to 1296 of the mRNA; GenBank accession no. J04018). The resulting plasmid, pDHFR-Luc-GFP (Fig. 1A), was linearized with NotI, and 50 μg of DNA was introduced into parasites by standard methods (23). After parasites were passaged sequentially for 2 weeks, tachyzoites that stably expressed GFP were isolated by fluorescence-activated cell sorting and were subsequently cloned by limiting dilution.

To determine the relative expression levels of luciferase in the *T. gondii* GFP-expressing clones, intracellular parasites of each clone were isolated by syringe lysis and quantified with a hemocytometer, and equal numbers of the parasites were serially diluted in 96-well plates with black walls (Costar, Corning, N.Y.). D-Luciferin potassium salt (Xenogen, Alameda, Calif.) was added to a concentration of 0.25 mg/ml, and the cultures were incubated for 10 min, after which each plate was directly imaged for 5 min with the Xenogen IVIS system (see below for a description of the IVIS imaging system and the image analysis software). The background settings were adjusted to 6,000 photons/s/cm^2/sr. These settings were the same settings used for all mouse imaging experiments (see below).

One clone of strain S23 (S23-luc7) and one clone of strain S22 (S22-luc2) had comparable luciferase expression levels (see below), and these clones were used in all subsequent experiments. Plasmid rescue was used to determine the site(s) of insertion of pDHFR-Luc-GFP in both strains as described previously (1). Briefly, genomic DNA was harvested from S23-luc7 and S22-luc2 by the TELT method (1), and 2 μg was digested in a 100-μl mixture with 20 U of SalI. Thirty nanograms of SalI-digested DNA was diluted to a concentration of 3 ng/μl and incubated overnight at 16°C with 2 U of T4 DNA ligase. One-half of the ligation reaction mixture was used to transform chemically competent *Escherichia coli*, and bacterial colonies carrying the plasmid were selected by growth on Luria-Bertani agar plates containing 100 μg of ampicillin per ml. For each strain, at least three colonies were examined by restriction digestion and sequencing. The insertion sites were identified by BLAST analysis of the rescued genomic sequence against the *T. gondii* genome (available at http://www.toxodb.org).

Growth competition assay. To determine if luciferase-expressing strains were impaired in their in vitro growth capacities, equal numbers of each luciferase-expressing strain and its wild-type counterpart were mixed and inoculated into

T25 flasks with HFFs. At the same time 100 parasites from the mixture were inoculated in triplicate into a 24-well plate with HFFs for a plaque (viability) assay. After lysis of a monolayer by the parasites, one-twentieth of the monolayer was transferred to another T25 flask. After 12 passages another plaque assay was performed, and the ratio of the different parasite strains (as determined by the presence or absence of GFP fluorescence) was calculated.

Infection of mice. Female BALB/c mice that were 5 to 10 weeks old (Jackson Laboratories, Bar Harbor, Maine) were used in all experiments. For intraperitoneal (i.p.) infection, S23-luc7 or S22-luc2 tachyzoites were grown in vitro and extracted from host cells by passage through a 27-gauge needle, and they were quantified with a hemocytometer. Parasites were diluted in phosphate-buffered saline, and mice were inoculated intraperitoneally with either 50 or 1,000 tachyzoites of each strain (in 100 μl) by using a 27-gauge needle. Since the viability of parasites isolated in this manner varied from batch to batch, plaque assays were performed with these preparations to determine the number of viable tachyzoites inoculated (4). Due to the comparatively high virulence of *T. gondii* clone S23-luc7, a subset of the mice infected intraperitoneally with S23-luc7 was given either 100 or 400 mg of sulfadiazine per liter in the drinking water during days 3 to 10 postinfection (p.i.) to facilitate survival of the mice beyond the acute stage of the infection (13).

Reactivation. Dexamethasone (DXM) was used to reactivate *T. gondii* according to the model developed by Djurkovic-Djakovic and Milenkovic (7). Dexamethasone (dexamethasone 21-phosphate disodium salt; Sigma) was dissolved at a concentration of 5 mg/liter in the drinking water. Treatment was started 80 days after infection. When no reactivation was seen after 25 days of treatment, the DXM concentration in the drinking water was doubled to 10 mg/liter.

In vivo imaging. The in vivo imaging system (IVIS; Xenogen, Alameda, Calif.), consisting of a cooled charge-coupled device camera mounted on a light-tight specimen chamber, a camera controller, a camera cooling system, and a Windows computer system, was used for data acquisition and analysis. D-Luciferin potassium salt (Xenogen), the substrate for firefly luciferase, was dissolved in phosphate-buffered saline at a concentration of 15.4 mg/ml and filtered through a 0.22-μm-pore-size filter before use. Mice were injected with 200 μl of luciferin (3 mg) and immediately anesthetized in an oxygen-rich induction chamber with 2% isofluorane. The mice were maintained for at least 10 min so that there was adequate dissemination of the injected substrate (5) and so that the animals were fully anesthetized. Mice were imaged in dorsal, ventral, and sometimes lateral positions by collecting two images, a grayscale reference image obtained under low-level illumination and an image of light emission from luciferase expressed in the parasites within the animals and transmitted through the tissue. Anesthesia was maintained during the entire imaging process by using a nose cone isofluorane-oxygen delivery device in the specimen chamber. Images were collected with 1- to 5-min integration times depending on the intensity of the bioluminescent signal, and pseudocolor representations of light intensity (red was the most intense, and blue was the least intense) were superimposed over the grayscale reference image. In certain cases mice were sacrificed after imaging, and individual organs were excised from the mice and imaged ex vivo. Data acquisition and analysis were performed by using the LivingImage (Xenogen) software with the IgorPro image analysis package (WaveMetrics, Seattle, Wash.). To allow comparisons between images from different days and different experiments, a background setting that could be applied to all images was determined empirically. Mice were injected with luciferin and imaged as described above, and the background cutoff of the images was adjusted so that no signal was detected in any of these control mice. The value obtained, 6,000 photons/s/cm^2/sr, was used as the background cutoff value for all images unless otherwise noted. The units of this value reflect the fact that the data were normalized with respect to imaging time, area imaged, and the distance between the light source (i.e., the mouse) and the charge-coupled device camera (5). For quantitation of the detected light over the course of infection, regions of interest were drawn by using IgorPro, and the light emitted from each region was recorded by recording the total number of photons per second (total flux).

RESULTS

Characterization of S23-luc7 and S22-luc2. To visualize *T. gondii* infection by bioluminescence imaging, it was necessary to engineer the parasite to express a luciferase gene. To do this, we used firefly luciferase, which Matrajt and colleagues have described previously as a heterologous reporter for this parasite (15). Several clones of each wild-type strain (S23 and S22) with stable expression of both GFP (as the selectable marker) and luciferase were isolated. One clone of each strain was chosen based on the production of comparable levels of light when the organisms were incubated with D-luciferin (S23-luc7 and S22-luc2) (Fig. 1B). We estimated the sensitivity of the imaging system for the detection of bioluminescent *Toxoplasma* strains in terms of the number of parasites necessary to detect a signal greater than the background signal in vivo. We injected mice intraperitoneally with 1×10^5, 1×10^4, or 1×10^3 S22-luc2 tachyzoites and imaged them 10 min later. Signals that were greater than the background signal in the abdomen were consistently detected only for mice injected with 1×10^5 tachyzoites (Fig. 1C).

Genomic sequences flanking the insertion site of the luciferase construct were determined for S23-luc7 and S22-luc2 by plasmid rescue, and the sequences were subjected to a BLAST analysis against the 9X version of the *T. gondii* genome (available at http://www.toxodb.org). For S23-luc7 the insertion was at position 2792490 of genomic scaffold TGG_995364, while in S22-luc2 the vector was inserted at position 448636 of genomic scaffold TGG_995285. For each strain at least three independent bacterial clones were found to contain the same genomic sequence, suggesting that only one copy of pDHFR-Luc-GFP was present in S23-luc7 and S22-luc2 and therefore that the insertions were at only one locus. Genomic sequences flanking the insertion sites were subjected to BLAST searches against the *T. gondii* expressed sequence tag (EST) database to determine if the insertion had disrupted any transcribed genes. The insertion in S23-luc7 was found to be in the 3′ UTR of the gene for ROP9 (after position 1711 of the gene; GenBank accession no. AJ401616), 386 bp downstream of the stop codon. The sequences near the insertion site for S22-luc2 were found to contain two expressed sequence tags, one ending 339 bp upstream of the insertion site (GenBank accession no. W06251) and the other starting 555 bp downstream of the insertion site (GenBank accession no. CN658789). When the insertion site was compared to a set of predicted polypeptides encoded by the *T. gondii* genome, it was found to be after the first base of predicted codon 101 of Twinscan-predicted protein 995285.056.1 (Twinscan2 predictions are available at http://www.toxodb.org). However, neither the EST sequences nor the Twinscan predicted protein was found to have significant BLAST homology (Expect > 10) to any characterized protein sequences in the GenBank database.

Comparisons of bioluminescent and wild-type strains. It was possible that insertion of the luciferase expression construct resulted in decreased fitness of the bioluminescent clones compared with their wild-type counterparts. Moreover, the different insertion sites of pDHFR-Luc-GFP could have resulted in phenotypic differences between S23-luc7 and S22-luc2. Therefore, we assessed both the in vitro growth capacities and the in vivo virulence phenotypes of these two strains compared to their nontransgenic parents. When cultures were initiated with equal numbers of S23-luc7 and S23 or with equal numbers of S22-luc2 and S22, the ratio of GFP-expressing parasites to wild-type parasites was approximately 1:3 after 12 in vitro passages. While this finding indicates that there was an approximately 10% difference in the amount of growth per passage between the bioluminescent and wild-type strains ($0.33^{1/12} = \sim 0.9$), this is a relatively minor disparity compared to the disparities for well-described fast-growing strains. For

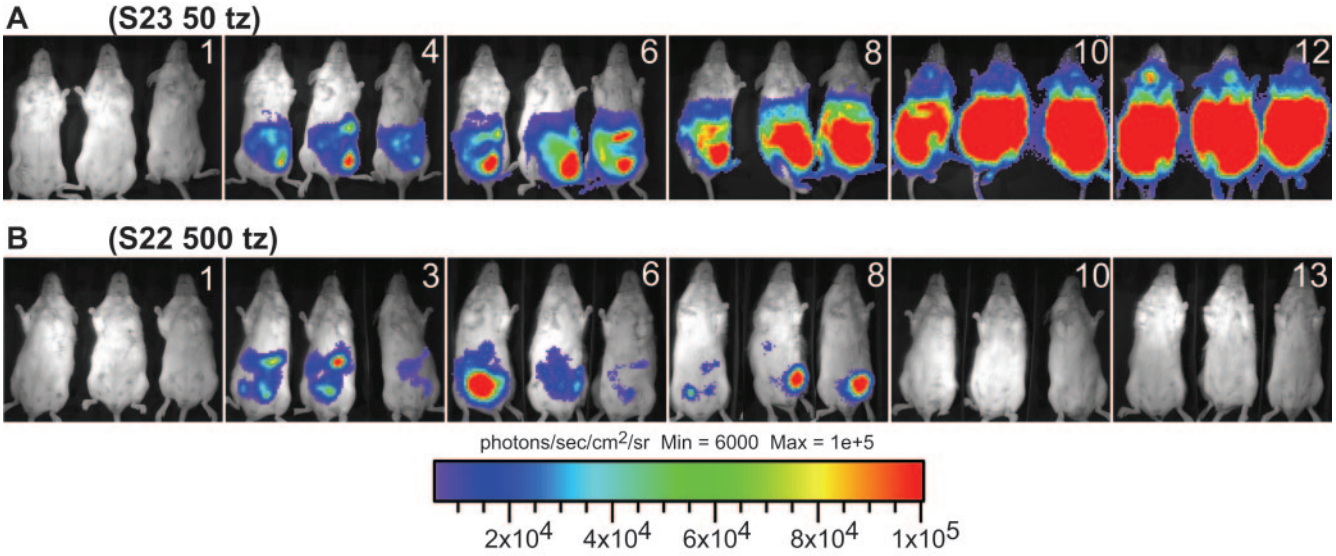

FIG. 2. Luminescent *T. gondii*, imaged on the days postinfection indicated with an IVIS imaging system (Xenogen). Tachyzoites (tz) were isolated from HFFs by syringe lysis, and BALB/c mice were infected with S23-luc7 (S23) (50 tachyzoites) or S22-luc2 (S22) (500 tachyzoites). Mice were imaged ventrally starting 1 day after infection, and the data are representative of two experiments (three mice per group). For all images shown, the color scale ranges from blue (just greater than the background noise; set to 6,000 photons/s/cm^2/sr) to red (at least 1×10^5 photons/s/cm^2/sr). (A) Typical course of i.p. infection of mice infected with *T. gondii* strain S23-luc7 (50 parasites). (B) Typical course of i.p. infection of mice infected with *T. gondii* strain S22-luc2 (500 parasites).

example, in similar cultures starting with a 50:1 ratio of either S23-luc7 or S22-luc2 to the rapidly growing type I strain RH, we could not detect any GFP-expressing parasites after 12 passages, as expected; i.e., RH fully outcompeted the luciferase-expressing strains. We also determined whether S23-luc7 retained the virulent phenotype of the wild-type strain and whether S22-luc2 retained the nonvirulent phenotype of the wild-type strain (9). In infections initiated in mice, injection of 50 S23-luc7 tachyzoites was uniformly lethal (three of three mice died from the infection; data not shown), while all five mice survived infection with 1,000 tachyzoites of S22-luc2. These results are highly consistent with the reported LD_{50}s for the wild-type S22 and S23 strains (9). Overall, these data suggest that the genetic manipulation necessary to express luciferase in S23 and S22 did not result in any significant alterations in the behavior of the organisms either in vivo or in vitro and therefore that S23-luc7 and S22-luc2 could be used as tools to infer differences between the wild-type strains during mouse infections.

Bioluminescence imaging of S23-luc7 and S22-luc2 reveals differences in dissemination. Our overall goal is to determine whether there are differences in dissemination between the virulent *Toxoplasma* strain S23 and the less virulent strain S22. To do this, we injected mice with bioluminescent *T. gondii* strains S23-luc7 and S22-luc2 and monitored the course of infection using an IVIS imaging system.

Figure 2 shows biophotonic images of three representative mice infected with either bioluminescent S23-luc7 (Fig. 2A) or bioluminescent S22-luc2 (Fig. 2B) over a 13-day i.p. infection. To obtain the data shown, mice were infected with approximately 50 S23-luc7 plaque-forming tachyzoites (Fig. 2A) or 500 S22-luc2 plaque-forming tachyzoites (Fig. 2B) based on a plaque assay. Both strains produced a significant bioluminescent signal in mice that allowed the progress of infection to be monitored noninvasively (no bioluminescence was observed in mice infected with either wild-type strain or in uninfected mice [data not shown]). In both the S23-luc7 and S22-luc2 infections, a bioluminescent signal was detectable by day 4 p.i., and it came exclusively from the abdomen. The mice infected with S23-luc7 shown in Fig. 2A illustrate the typical disease progression that we observed in infections with this virulent strain. The amount of signal detected in the abdomens of S23-luc7-infected mice increased over the course of the infection (Fig. 2A), and quantitative analysis showed that the increase was exponential during days 1 to 10 (Fig. 3). In addition, signals were detected in the thorax and neck on days 10 and 12. All three mice in this group succumbed to the infection on day 13 or 14.

The course of the infection with nonvirulent S22-luc2 was dramatically different from the course observed for virulent S23-luc7 (Fig. 2B). For mice infected with 5 or 50 S22-luc2 tachyzoites there was a signal only at the site of injection (data not shown). For the mice infected with 500 S22-luc2 tachyzoites a bioluminescent signal greater than the background signal was observed in the peritoneal cavity at day 3 p.i., and this signal increased by day 6 (Fig. 2B and 3). By day 10, however, a signal was no longer detectable. In these mice we never observed signal in any area except the abdomen, and after day 8 we never observed a signal greater than the background signal anywhere in these mice. None of the mice infected with S22-luc2 died. Thus, using bioluminescence imaging, we could detect dramatic differences in growth and dissemination between the virulent S23-luc7 strain and the less virulent S22-luc2 strain.

Mice were also infected with a lower dose of S23-luc7, and by using the plaque assay it was determined that these mice

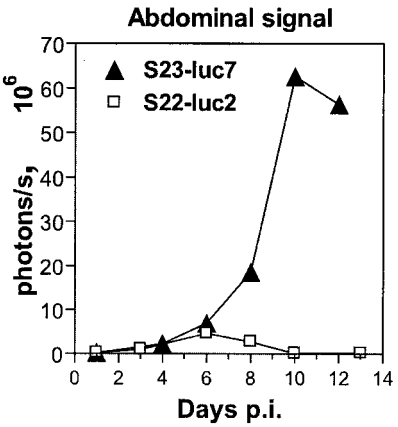

FIG. 3. Course of infection with luciferase-expressing *T. gondii* strains expressed in terms of the photonic signal. Mice were infected intraperitoneally with either 50 S23-luc7 tachyzoites or 500 S22-luc2 tachyzoites and imaged three times per week. The images were analyzed by measuring the total light flux (number of photons per second) coming from the abdominal cavity, and the data points are the averages for three mice per strain. The emitted signal from the S23-luc7-infected mice increased exponentially during days 4 to 10. In contrast, the detected light from S22-luc2-infected mice peaked at day 6 and began to decrease soon after this, and the level was below the background level by day 10 p.i.

were injected with approximately five plaque-forming tachyzoites. One of the mice in this group died 14 days p.i., and the course of infection was very similar to that of the mice infected with 50 S23-luc7 tachyzoites (data not shown). Two mice in this experiment survived the acute phase of the infection with S23-luc7, and the time course of the infection is shown in Fig. 4A. In one S23-luc7-infected mouse, the bioluminescent signal in the abdomen peaked at day 10 and then progressively decreased during days 12 to 14 (Fig. 4A). When this mouse was imaged again on day 18, a signal was no longer detected in the peritoneal cavity, but there was a signal from the thorax, head, and what seemed to be the eyes. By dissection of a similar mouse in another experiment, the thorax signal was determined to be due to extensive infection of the lungs, as expected (18). The lung signal was not detected on day 25 p.i. The head signal was still present on day 25 p.i., but it was not detected on day 32 p.i. or during later imaging sessions. Another mouse died at day 29 p.i., presumably from encephalitis.

In mice infected with S23-luc7, a characteristic signal in a region around the neck was visible within 24 h before death (Fig. 2A, day 12). After dissection of one such mouse, this signal was found to come from the superficial cervical lymph nodes (Fig. 4C). In addition, after dissection, bioluminescent

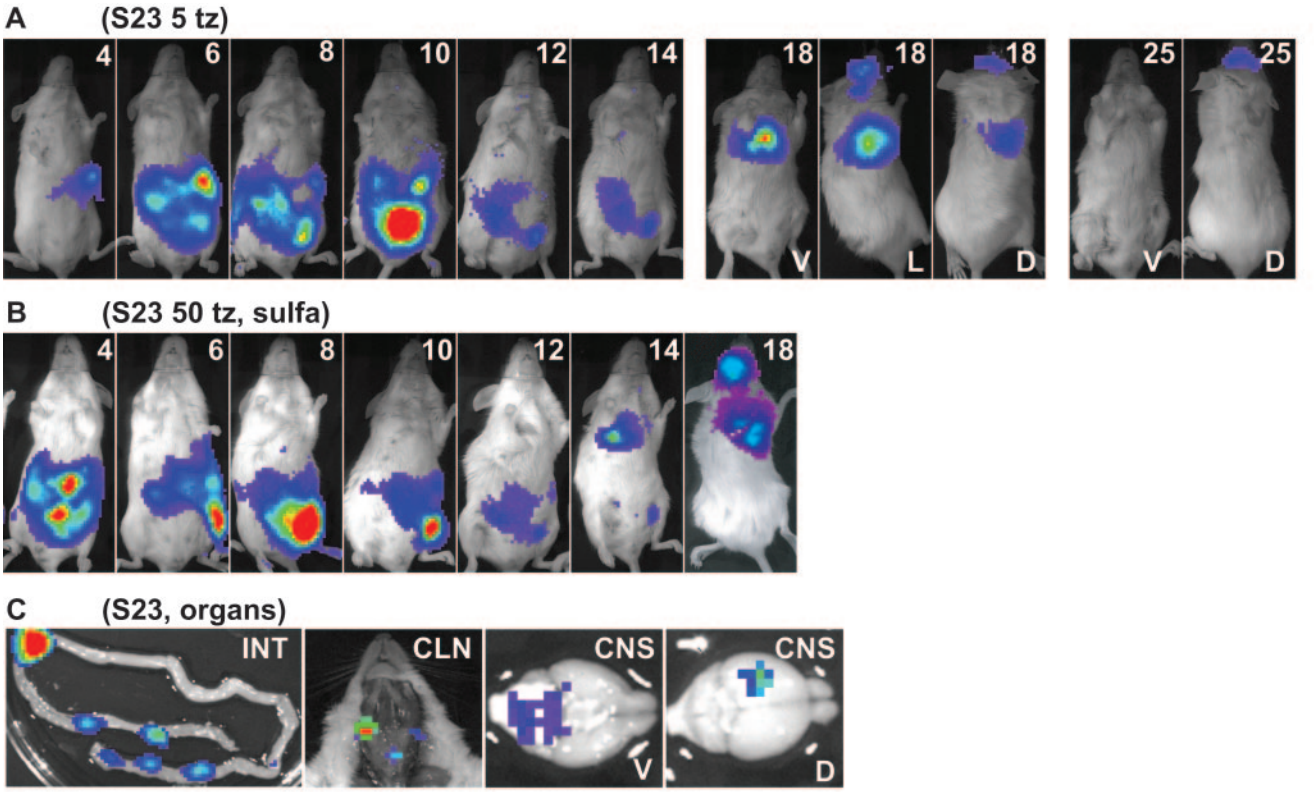

FIG. 4. (A) Course of i.p. infection of a mouse that survived infection with *T. gondii* strain S23-luc7 (five parasites). One ventral image is shown for days 4 to 14, while for days 18 and 25 ventral (V), lateral (L; day 18 only), and dorsal (D) images (of the same mouse) are shown. The color scale for the images is the same as that in Fig. 2. (B) Course of i.p. infection in a mouse infected with *T. gondii* strain S23-luc7 (50 parasites) and treated from day 3 to 10 with 100 mg of sulfadiazine per liter. Ventral images taken on days 4 to 18 are shown. The color scale for the images is the same as that in Fig. 2. (C) Organs dissected from a mouse infected with 50 S23-luc7 parasites on day 13 p.i. (without sulfadiazine treatment). In the image of the small intestine (INT), much of the signal comes from discrete patches. Signals were also observed in images of the cervical lymph nodes (CLN) and in ventral (V) and dorsal (D) views of the brain (CNS). Given the increased sensitivity of imaging of infected organs ex vivo, background settings were adjusted for these images to allow the most intense signal sources to be visualized in the context of the entire organ. Abbreviations: S23, S23-luc7; tz, tachyzoites; sulfa, sulfadiazine.

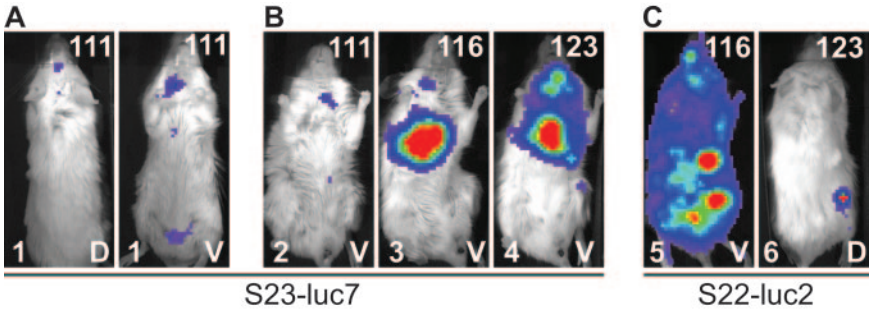

FIG. 5. Reactivation of *Toxoplasma* in mice infected with either S23-luc7 (A and B) or S22-luc2 (C). Immunosuppressive therapy was started 80 days after infection by adding dexamethasone sulfate (5 mg/liter) to the drinking water. At day 105 p.i. the dose was doubled to 10 mg/liter. In all images, the number of days postinfection is indicated in the upper right corner, the mouse number is indicated in the lower left corner, and the view (dorsal [D] or ventral [V]) is indicated in the lower right corner. (A) Dorsal and ventral views of reactivation 111 days p.i. in a mouse infected with five S23-luc7 tachyzoites (not treated with sulfadiazine). The signal was observed first in the head, abdomen, and cervical lymph nodes. The two images are images of the same mouse. (B) Reactivation in three different mice (mice 2, 3, and 4) infected with S23-luc7 and treated with sulfadiazine (100, 400, and 400 mg/liter, respectively) during the acute phase of infection. After reactivation, the signal was first observed in all three mice in the cervical lymph nodes, and signal was also detected in the lungs in mice 3 and 4. (C) Examples of reactivation in mice infected with S22-luc2. Mouse 5 was imaged ventrally, and mouse 6 was imaged dorsally. Reactivation occurred primarily in the peritoneal cavity in mouse 5, while it was restricted to the right thigh in mouse 6.

signals were detected in many other organs, including, in descending order of total light flux, the intestine (6×10^7 photons/s, mainly from discrete patches) (Fig. 4C), the lungs (1×10^7 photons/s), the liver (1×10^7 photons/s), peritoneal cells (7×10^6 photons/s from 2.6×10^6 cells), the spleen (4×10^6 photons/s), the kidneys (4×10^5 photons/s), the brain (4×10^5 photons/s), and the heart (3×10^5 photons/s).

Real-time monitoring of anti-*Toxoplasma* therapy. Sulfadiazine, an inhibitor of folic acid synthesis, is effective in treating *Toxoplasma* infections in mouse models and human patients. To determine whether bioluminescence imaging can be used to monitor the efficacy of anti-*Toxoplasma* therapy in real time, we monitored the effect of early sulfadiazine treatment of mice infected with the virulent S23-luc7 strain. Mice were injected with a high, normally lethal inoculum (50 parasites) or a low inoculum (5 parasites) and treated with 100 or 400 mg of sulfadiazine per liter in the drinking water. Treatment started on day 3 and continued through day 10. With both the high and low doses of the drug and with either inoculum, all mice survived the acute phase of infection up to day 18. Figure 4B shows the typical course of infection of a mouse infected with 50 S23-luc7 tachyzoites and treated with 100 mg of sulfadiazine per liter. Bioluminescence was detected only in the abdomen during days 4 to 12, and from day 14 to day 18 a strong signal was also seen in the thorax and head; based on dissection of a similar mouse in another experiment, these signals came from the lungs and the brain, respectively. Two mice infected with 50 S23-luc7 tachyzoites died at 20 and 25 days p.i., while one mouse infected with 5 S23-luc7 tachyzoites died at 24 days p.i.

With the high dose of sulfadiazine, no signal was detected from day 8 onward in mice infected with five S23-luc7 tachyzoites (data not shown). In mice infected with 50 S23-luc7 tachyzoites, the signal disappeared from the abdomen after day 8, and the only signal detected after this was a signal in the head (brain) during days 14 to 25 (data not shown). None of the mice treated with the high dose of sulfadiazine died. These results show that bioluminescence is an effective way to monitor the efficacy of a drug over and above simple survival curves.

Immunosuppression reveals distinct sites of reactivation of S23-luc7 and S22-luc2. Mice that survived a previous infection were immunosuppressed with DXM to assess if either drug treatment or the immune system had cleared all parasites and, if all parasites had not been cleared, to monitor the course of reactivation. Immunosuppression was begun 80 days after infection by adding a water-soluble form of DXM to the drinking water. Reactivation was monitored by imaging treated mice regularly. No bioluminescence was detected after 25 days of treatment, and so the dose of DXM was doubled. Six days after this, the first signs of reactivation were seen in mice that had been infected with S23-luc7 (day 111) (Fig. 5A and B). Interestingly, while a weak signal was observed in the head region (Fig. 5A) in some mice, reactivation in S23-luc7-infected mice started mainly in the lungs (confirmed after dissection) and cervical lymph nodes (Fig. 5B). However, after dissection, parasites were also detected in the brain (as expected) and the intestine in these mice. Interestingly, in the two cases in which reactivation was seen with S22-luc2, the signal appeared in an area that was different from the area in which the S23-luc7 signal was seen. In one mouse (mouse 5) (Fig. 5C), the most intense signal was seen in the peritoneal cavity, although the fact that a signal came from nearly every part of this mouse suggests that it had an extremely high parasite burden. In another mouse infected with S22-luc2 that reactivated (mouse 6) (Fig. 5C), the most intense signal was detected in an area near the thigh. Thus, bioluminescence allowed the anatomical sites of *Toxoplasma* reactivation induced by oral administration of DXM to be observed. Moreover, the results revealed differences that appear to be strain specific, although more mice need to be examined before this conclusion can be drawn with confidence.

DISCUSSION

In this study, we demonstrated the use of photonic imaging to visualize bioluminescent *Toxoplasma* in live animals. We found that differences due to strain and/or treatment can be

effectively observed with fewer animals and with much greater precision and subtlety than when previously described methods are used. While head-to-head comparisons of the dissemination patterns of different *T. gondii* strains and of the pharmacodynamics of anti-*Toxoplasma* drugs have been made by other workers, these workers have routinely relied on plaque assays and quantitative PCR with tissue homogenates to determine parasite burdens in organs of interest (10, 17). While useful, these methods have several disadvantages. First, the animal analyzed must be sacrificed, and, therefore, it is not possible to monitor the kinetics and extent of disease progression in the same animal over time. This obscures the true pattern of infection and also means that significant insights from animal-to-animal variations may be missed. It also means that many more animals must be used to obtain convincing data if multiple times are to be examined. Second, the traditional methods are laborious and depend on knowing which tissue to examine; dissemination to unexpected anatomical sites or even to particular subcompartments of the organ being examined may easily be missed. Third, they are dependent on obtaining reproducible, quantitative recovery of the parasites and on there being no variation in the efficiency of amplification or plating.

The nondestructive and noninvasive nature of bioluminescent imaging overcomes many of these problems. For example, the procedure can be performed repeatedly, which allows each animal to be used as its own control. Thus, averaging effects are eliminated at the same time that the overall number of animals required is greatly reduced. The noninvasive approach described here is significantly more rapid than conventional techniques and should not be subject to variations in recovery or to sampling of an organ that is not the actual focus of infection in an animal. In the present study we observed remarkable differences in dissemination between two *T. gondii* strains (S22-luc2 and S23-luc7) that was apparent by day 8 p.i. Given the large differences in the virulence of these two sibling strains, this dissemination pattern could serve as an early indicator of the eventual outcome of the infection. Of course, there are limitations to this approach. First, while *T. gondii* is highly amenable to genetic manipulation, it is not trivial to engineer strains that stably express GFP and luciferase, and there is no way to be absolutely sure that the resulting strains have no phenotypic differences from the wild-type strains. In these experiments, we found an extremely small difference in growth in vitro, and both the bioluminescent strains had LD_{50}s in the previously published range, suggesting that the luciferase and GFP had little if any effect in vivo. The genomic insertion site could also affect the phenotype independent of the luciferase gene, but again we saw no evidence of this in these experiments. The potential problem of a phenotypic effect of the insertion site could be solved either by using multiple strains with insertions in different loci or by targeting the insertion to the same, neutral locus in all strains. Second, for detection of parasites in a tissue of interest, our assay is much less sensitive than plaque assays or PCR, both of which have a potentially lower limit of detection (a single organism). This limitation can be partially overcome by sacrificing the animal and exposing the organs, which results in a substantial increase in sensitivity but obviously ends the time course with that animal unless the study is done with nonlethal, surgical procedures. Third, the sensitivity varies from organ to organ, since different tissues absorb the light with different efficiencies and it is estimated that each centimeter of tissue lowers the detectable bioluminescent signal 10-fold (5). This limitation is also partly overcome by opening the animal up (5).

A good example of the added value of bioluminescent imaging was apparent when mice were injected with a low dose (five parasites) of S23-luc7. Because each mouse could be monitored individually over time, we were able to see the individual differences between mice surviving the infection and mice that were about to die (Fig. 2A and B and 4A and B). Interestingly, all S23-luc7-infected mice that died in the acute phase developed a signal around the ventral side of the neck, and after dissection this signal was shown to be coming from the cervical lymph nodes (Fig. 4C). This provides important clues concerning the fatal pathogenesis in this model. This is similar to the situation in humans, where lymphadenopathy, primarily of the cervical type, is one of the most common signs of symptomatic, acquired toxoplasmosis (16).

The advantages and disadvantages of the technique are also apparent in the analysis of brain infection in animals infected with S23-luc7. Although no head signal could be seen in living mice at day 13, dissection of the same animals showed a clear signal in the brain (Fig. 4C). Moreover, once the brain was dissected, the signal could be seen to be coming from specific parts of the brain. This degree of resolution could be critical when the neurobiology of *Toxoplasma* infection is studied, as it allows correlations to be made between particular symptoms and the focus of the infection in the brain (e.g., in the well-described phenomenon of inhibition of neophobia in rats by *Toxoplasma* [3, 25, 26]). These results also show the danger of using one side of the brain for plaque assays and the other side for initiating an oral infection and assuming that the same numbers of parasites are present.

The bioluminescence detected in mice infected with S22-luc2 was contained in the peritoneal area, and the signal disappeared abruptly and completely between day 8 and day 10, presumably due to an effective immune response. However, because the firefly luciferase gene was cloned behind the *Toxoplasma* DHFR promoter, the loss of signal could also be explained by a loss of promoter activity for this gene (e.g., because the parasites had switched from the tachyzoite stage to the bradyzoite stage). Consistent with this, all ESTs for DHFR are from tachyzoite libraries, suggesting that the DHFR promoter is specific for this parasite stage. If this is true, the luciferase expression might be turned off upon stage conversion. This limitation could be overcome by using a constitutive promoter, although metabolic differences between the two forms might still give different sensitivities of detection. On the other hand, this phenomenon could be exploited to distinguish between the two asexual forms of the parasite by, for example, engineering parasites to express luciferase driven by a bradyzoite-specific promoter. Ultimately, it may prove to be possible to engineer strains in which luciferases which use different substrates (e.g., luciferases from firefly and renilla) are under control of tachyzoite- or bradyzoite-specific promoters in order to simultaneously distinguish the two forms.

Bioluminescent imaging of *Toxoplasma* infection was probably most valuable in the studies reported here when reactivation was investigated. After the start of treatment, it is difficult

to know if the parasites have reactivated until symptoms are observed or the animal is sacrificed. Immunosuppressive therapy itself can result in the death of control animals, making it difficult to know if an infected animal died of toxoplasmosis or from side effects of the treatment (7). This problem is overcome by imaging which clearly indicates where, when, and to what degree reactivation is occurring. Hence, by using these methods it could be feasible to assess not only the effects of a given drug on tachyzoite multiplication and dissemination but also the effects on the parasite's ability to encyst, lie dormant, and reactivate. Currently, no drugs give a sterile cure, and this method may help in the discovery of such drugs.

Finally, there are some clear trends in our results that shed new light on the pathogenesis of this parasite and the differences between strains. For example, it is apparent that the highly virulent S23 strain disseminates in much larger numbers to far more tissues than the S22 strain. Although not directly demonstrated, this increased dissemination is almost certainly a major factor in the virulence of the S23 strain. Second, the major focus of reactivation can be seen to be in different locations in different animals, despite identical infection and treatment regimens. More animals need to be studied, but it is likely that while the site of reactivation is animal specific, it may also be influenced by strain type.

ACKNOWLEDGMENTS

We thank Chris Contag, Timothy Doyle, and Jonathan Hardy for many helpful discussions.,

REFERENCES

1. **Arrizabalaga, G., F. Ruiz, S. Moreno, and J. C. Boothroyd.** 2004. Ionophore-resistant mutant of *Toxoplasma gondii* reveals involvement of a sodium/hydrogen exchanger in calcium regulation. J. Cell Biol. **165:**653–662.
2. **Barragan, A., and L. D. Sibley.** 2002. Transepithelial migration of *Toxoplasma gondii* is linked to parasite motility and virulence. J. Exp. Med. **195:**1625–1633.
3. **Berdoy, M., J. P. Webster, and D. W. Macdonald.** 2000. Fatal attraction in rats infected with *Toxoplasma gondii*. Proc. R. Soc. Lond. B Biol. Soc. **267:**1591–1594.
4. **Camps, M., and J. C. Boothroyd.** 2001. *Toxoplasma gondii*: selective killing of extracellular parasites by oxidation using pyrrolidine dithiocarbamate. Exp. Parasitol. **98:**206–214.
5. **Contag, C. H., P. R. Contag, J. I. Mullins, S. D. Spilman, D. K. Stevenson, and D. A. Benaron.** 1995. Photonic detection of bacterial pathogens in living hosts. Mol. Microbiol. **18:**593–603.
6. **Darcy, F., and F. Santoro.** 1994. Toxoplasmosis, p. 163–201. *In* F. Kierszenbaum (ed.), Parasitic infections and the immune system. Academic Press, New York, N.Y.
7. **Djurkovic-Djakovic, O., and V. Milenkovic.** 2001. Murine model of drug-induced reactivation of *Toxoplasma gondii*. Acta Protozool. **40:**99–106.
8. **Gavrilescu, L. C., and E. Y. Denkers.** 2001. IFN-gamma overproduction and high level apoptosis are associated with high but not low virulence *Toxoplasma gondii* infection. J. Immunol. **167:**902–909.
9. **Grigg, M. E., S. Bonnefoy, A. B. Hehl, Y. Suzuki, and J. C. Boothroyd.** 2001. Success and virulence in *Toxoplasma* as the result of sexual recombination between two distinct ancestries. Science **294:**161–165.
10. **Jauregui, L. H., J. Higgins, D. Zarlenga, J. P. Dubey, and J. K. Lunney.** 2001. Development of a real-time PCR assay for detection of *Toxoplasma gondii* in pig and mouse tissues. J. Clin. Microbiol. **39:**2065–2071.
11. **Johnson, W. D., Jr.** 1981. Chronological development of cellular immunity in human toxoplasmosis. Infect. Immun. **33:**948–949.
12. **Joiner, K. A., and J. F. Dubremetz.** 1993. *Toxoplasma gondii*: a protozoan for the nineties. Infect. Immun. **61:**1169–1172.
13. **Kong, J. T., M. E. Grigg, L. Uyetake, S. Parmley, and J. C. Boothroyd.** 2003. Serotyping of *Toxoplasma gondii* infections in humans using synthetic peptides. J. Infect. Dis. **187:**1484–1495.
14. **Luft, B. J., and J. S. Remington.** 1992. Toxoplasmic encephalitis in AIDS. Clin. Infect. Dis. **15:**211–222.
15. **Matrajt, M., M. Nishi, M. J. Fraunholz, O. Peter, and D. S. Roos.** 2002. Amino-terminal control of transgenic protein expression levels in *Toxoplasma gondii*. Mol. Biochem. Parasitol. **120:**285–289.
16. **Montoya, J. G., and O. Liesenfeld.** 2004. Toxoplasmosis. Lancet **363:**1965–1976.
17. **Mordue, D. G., F. Monroy, M. La Regina, C. A. Dinarello, and L. D. Sibley.** 2001. Acute toxoplasmosis leads to lethal overproduction of Th1 cytokines. J. Immunol. **167:**4574–4584.
18. **Pomeroy, C., and G. A. Filice.** 1992. Pulmonary toxoplasmosis: a review. Clin. Infect. Dis. **14:**863–870.
19. **Roos, D. S., R. G. Donald, N. S. Morrissette, and A. L. Moulton.** 1994. Molecular tools for genetic dissection of the protozoan parasite *Toxoplasma gondii*. Methods Cell Biol. **45:**27–63.
20. **Sibley, L. D., and J. C. Boothroyd.** 1992. Virulent strains of *Toxoplasma gondii* comprise a single clonal lineage. Nature **359:**82–85.
21. **Sibley, L. D., A. J. LeBlanc, E. R. Pfefferkorn, and J. C. Boothroyd.** 1992. Generation of a restriction fragment length polymorphism linkage map for *Toxoplasma gondii*. Genetics **132:**1003–1015.
22. **Sims, T. A., J. Hay, and I. C. Talbot.** 1989. An electron microscope and immunohistochemical study of the intracellular location of *Toxoplasma* tissue cysts within the brains of mice with congenital toxoplasmosis. Br. J. Exp. Pathol. **70:**317–325.
23. **Soldati, D., and J. C. Boothroyd.** 1993. Transient transfection and expression in the obligate intracellular parasite *Toxoplasma gondii*. Science **260:**349–352.
24. **Su, C., D. Evans, R. H. Cole, J. C. Kissinger, J. W. Ajioka, and L. D. Sibley.** 2003. Recent expansion of *Toxoplasma* through enhanced oral transmission. Science **299:**414–416.
25. **Webster, J. P.** 2001. Rats, cats, people and parasites: the impact of latent toxoplasmosis on behaviour. Microbes Infect. **3:**1037–1045.
26. **Webster, J. P., C. F. Brunton, and D. W. MacDonald.** 1994. Effect of *Toxoplasma gondii* upon neophobic behaviour in wild brown rats, *Rattus norvegicus*. Parasitology **109:**37–43.

Editor: J. F. Urban, Jr.